Measurement of Humidity Profiles in the Atmosphere by the Global Positioning System and Radar Wind Profilers

EARL E. GOSSARD

Science and Technology Corporation/NCAA/Environmental Technology Laboratory, Boulder, Colorado

DANIEL E. WOLFE AND B. BOBA STANKOV

NOAA/ERL/Environmental Technology Laboratory, Boulder, Colorado

30 December 1997 and 26 March 1998

ABSTRACT

Bragg backscatter of radar waves from elevated turbulent layers is very highly correlated with the height profile of the gradient of radio refractive index through elevated turbulent layers, as has often been documented in past research. However, many users need profiles of radio refractive index or the associated humidity rather than profiles of their gradients. Simple integration of the gradients is usually not feasible because clutter and various noise sources often severely contaminate the lower-range gates. The authors show that if the total integrated humidity is independently available [for example, from the Global Positioning System (GPS)] and if the surface value of humidity is known, the profiles of humidity are retrievable with good accuracy. This method is demonstrated with data collected in Southern California, where 7 h of 449-MHz data were recorded along with GPS data. Three radiosonde balloons were launched during that period, and the profiles of humidity from the two sources are compared. Simulations are used to assess errors that result from factors such as lack of the sign of the humidity gradients. In conclusion, a humidity profile found by statistical retrieval is compared with one found by the technique proposed in this paper.

1. Introduction

The close relationship between refractive-index gradients with height and the distribution of Bragg backscattered power with height has been noted for decades; for example, see Fig. 1 taken from Richter and Gossard (1970) [see also Ottersten (1969); Bean et al. (1971); Chadwick and Gossard (1983)]. The refractive index at microwave frequencies depends mainly on temperature and humidity (and weekly pressure) (e.g., Bean and Dutton 1966). Therefore, if the profiler can provide the refractive-index gradient and if temperature is available from a radio acoustic sounding system (RASS), the calculation of humidity gradients is straightforward. In the San Diego experiment, described herein, RASS soundings were available.

For several reasons, simple integration has not been practical for converting the gradients into profiles. Difficulties include the often severe contamination by various forms of clutter in the lower gates where the integration is initiated, the loss of sign in the conversion of backscatter power to the humidity gradient (because the squared gradient of refractive index is deduced from backscattered power), and the need for noisy measurements of Doppler spectral second moments and wind shear squared. In past papers (e.g., Gossard et al. 1998, hereafter referred to as GWMPAR), we argued that a practical use for the profiler data was to assimilate the humidity gradient information into models. However, the new availability of temperature sounding with RASS and the imminent availability of global total precipitable water vapor (PWV) from the Global Positioning System (GPS) suggest a reassessment of profilers as sensors of humidity profiles as well as of humidity gradient profiles. The purpose of the San Diego experiment was to evaluate this concept of humidity retrieval.

The Southern California area was chosen for our experiment because the large ranges in temperature and humidity commonly found in the profiles allow large amounts of data to be collected in a short time. Thus, the method can be tested over the entire range of variation of the properties. In this experiment, the large temperature inversion was often so low and intense that the gradients of interest were within the lower few gates (300–600 MSL) of the radar, where there were many extraneous targets and much clutter. On 27 September 1995 the inversion was between 700 and 1000 m (see Fig. 2), so the height range of interest was uncontam-

Corresponding author address: Dr. Earl E. Gossard, NOAA/ETL, R/E/ET4, 325 Broadway, Boulder, CO 80303.
E-mail: egossard@ett.noaa.gov

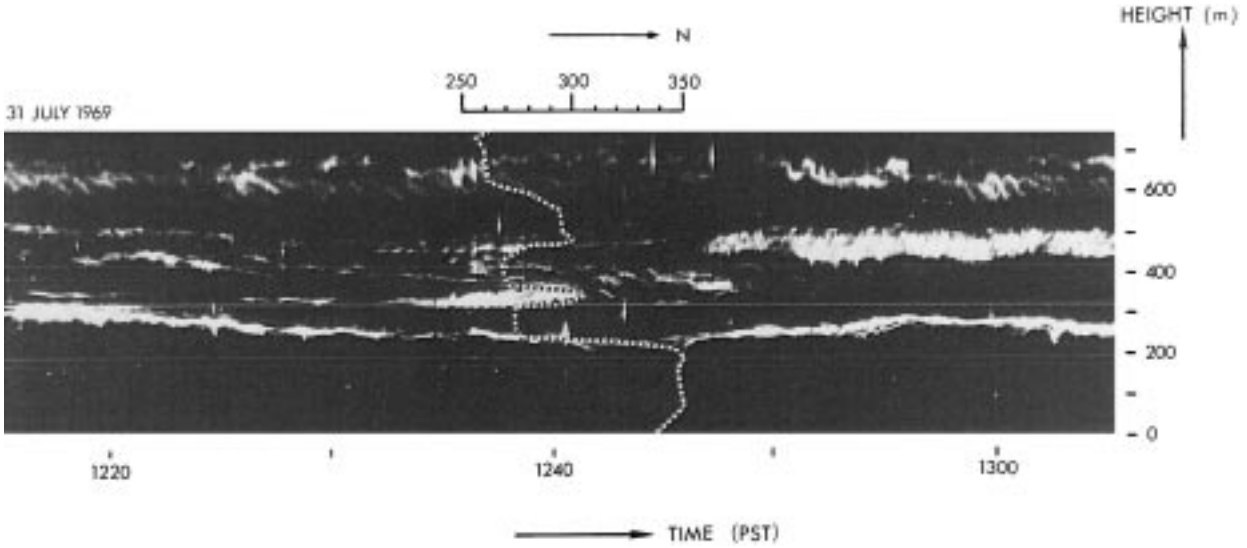

FIG. 1. Multilayer backscatter observed with an FM–CW radar at San Diego compared with a balloon sounding (dashed) of radar refractive index from a launch at 1238 PST. The very close relationship between radar backscatter and refractive-index gradient (and therefore humidity) is illustrated (from Richter and Gossard 1970).

inated. For this reason, that day was examined in detail by GWMPAR, and we examine it further here.

2. Theory

The conceptual relationship between gradient quantities and turbulence properties is given by Tatarskii (1971) and Ottersten (1969). The radar profiling applications were formulated by VanZandt et al. (1978) and Gage and Balsley (1980). The results can be written as in GWMPAR:

$$\left[\frac{d(N_p)}{dz}\right]^2 \simeq \left(\frac{B_w}{B_N}\right)(\mathrm{Pr} - \mathrm{Ri})\left(\frac{du_0}{dz}\right)^2\frac{C_N^2}{C_w^2}$$

$$= \left(\frac{L_w}{L_N}\right)^{4/3}\left(\frac{du_0}{dz}\right)^2\frac{C_N^2}{C_w^2}. \qquad (1)$$

The form on the right side of (1) and its implication for a Pr versus Ri relationship was noted by Gossard et al. (1982), and this relationship was used by GWMPAR. In (1), z is height; u_0 is the mean wind speed; Pr is the turbulent Prandtl number; Ri is the gradient Richardson number; B_w and B_N are Kolmogorov constants, C_w^2 is the turbulent structure parameter of vertical velocity, w; and C_N^2 is the structure parameter of potential refractive index, N_p. The potential refractive index depends on temperature and humidity and is the radar refractive index expressed in potential temperature and absolute humidity. The radar senses the structure parameter of the refractive index rather than the potential refractive index. Therefore, in dealing with profiles, the conversion of the structure parameter N to that of potential refractive index is significant (Gossard and Strauch 1983, appendix B). It is referenced to a pressure level of 1000 mb and thus is conserved in a clear-air parcel undergoing adiabatic translation. The ''length scales'' (e.g., Tatarskii 1971, 72) of the refractive-index field and vertical velocity field are L_w and L_N, respectively. These length scales are not, in general, equal and are highly variable, but Gossard et al. (1982) argue that their ratio (L_w/L_N) might be expected to be a fairly conservative property because refractive index and momentum are mixed by the same turbulence ensemble regardless of stability, shear, etc. Gossard et al. (1982) pointed out that this assumption leads to a reasonable relationship between Pr and Ri. GWMPAR measured the critical length scales from mixed radar and balloon data. The scales had much scatter, but their ratio had a median value of about 4, independent of stability. We expect that factors such as anisotropy and nonstationarity may degrade the constancy of the ratio.

We found, especially in the lower few range gates, that it is important to edit the spectra carefully when evaluating C_N^2 to ensure that the power (zero moment) and first moment are from atmospheric backscatter *only* and are not contaminated by any of the various clutter sources.

GWMPAR focused on the measurement of the quantities in the proportionality factor in (1), especially the measurement of C_w^2 using the second moment (width) of the Doppler spectrum. Gradients of N_p were then calculated from (1), and the corresponding values of $d\rho_V/dz$ were found from the N_p gradients and RASS temperature gradients using the well-known relationship among temperature, humidity, and refractive index for microwave frequencies (e.g., see Bean and Dutton 1966). The gradients calculated by GWMPAR agreed well with the balloon-measured gradients of ρ_V and N_p

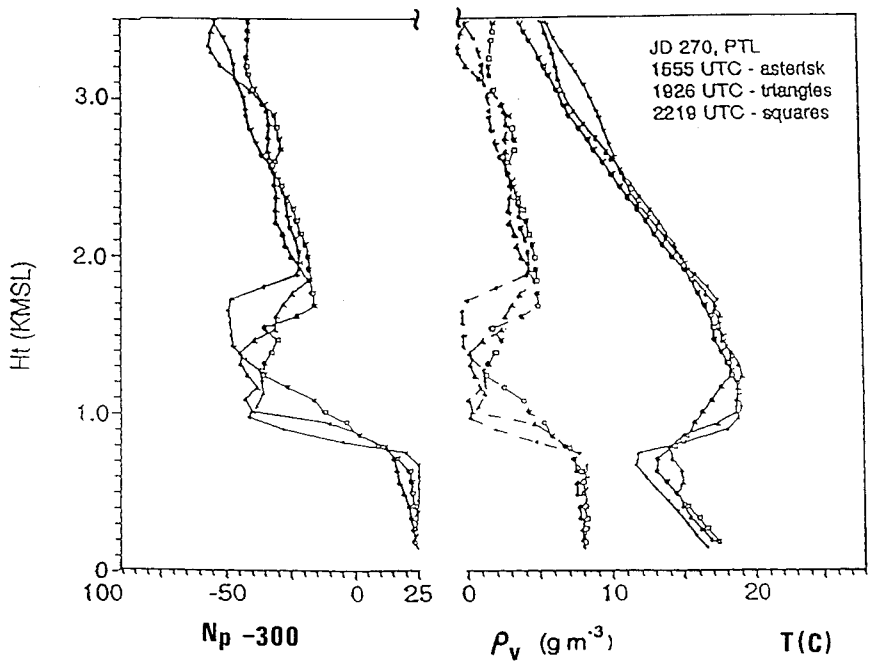

FIG. 2. Profiles of temperature, humidity, and refractive index on 27 September 1995 (JD 270), at Point Loma from balloon launches at 1556, 1926, and 2219 UTC.

and are used in this paper to derive radar-retrieved profiles of N_p and ρ_V. Using the new availability of GPS values of PWV, we decided to test a procedure to retrieve the humidity and refractive-index profiles (rather than only profiles of the gradients). We constrained the integration of the gradients to yield the total N_p corresponding to the total PWV found from GPS. The optimum profile of N_p was found iteratively. This procedure leads to a new estimate of the proportionality factor in (1). If the new factor leads to profiles that agree well with balloon observations, it implies that the error is independent of height and resides mainly in our estimate of the ratio $(L_w/L_N)^{4/3}$.

Note that the above solutions of the direct retrieval problem are somewhat analogous to the indirect retrieval of the humidity profile by the statistical inversion demonstrated by Stankov et al. (1996). In that paper, the retrieval used local climatology and microwave radiometric data from Erie, Colorado, with mathematical inversion in order to obtain a humidity profile. That profile was then further constrained by profiler-deduced humidity gradients in order to improve the humidity profile estimates. The result agreed well with local Denver, Colorado, balloon soundings. The two techniques are compared in section 6.

3. Measurements

Figure 2 shows balloon soundings of (a) potential (radio) refractive index (N_p), (b) humidity [ρ_V (g m^{-3})], and (c) air temperature [T (°C)] for 0900, 1226, and 1519 LT 27 September 1995. In the top frame of Fig. 3 the cumulative percent of PWV versus height is shown. The three curves have been calculated from the balloon soundings for comparison with the GPS total PWV, which was independently measured with a GPS receiver at the balloon launch site. We assumed that the three curves were representative of the climate over San Diego under these meteorological conditions. The bottom frame of Fig. 3 shows the temporal history of the surface humidity and the PWV from GPS on this day. The 449-MHz profiler described by Wolfe et al. (1997) was located about 300 m from the balloon launch site. The profiler is a five-beam system cycling successively through vertical and through radials 15° off-vertical with the bearings at north, south, east, and west in about 3.1 min. It takes about 10 min for the balloon to rise to the height of maximum penetration of the RASS acoustic signal. Therefore, the radar provided three profiles during the balloon's ascent.

4. Data analysis

This data analysis requires a calibrated, five-beam wind profiler with attention to effective sidelobe reduction. In our case, the profiler was located in a deep gully. It was necessary to edit the spectra rather than the spectral moments, as is usually done. Therefore, a large part of the effort in this program was devoted to the development of software to automatically choose the spectral components that are due to atmospheric backscatter, while rejecting ''noise'' from aircraft, birds, ground and sea clutter, and radio frequency interference. In this effort, software was developed using the cross-correlation

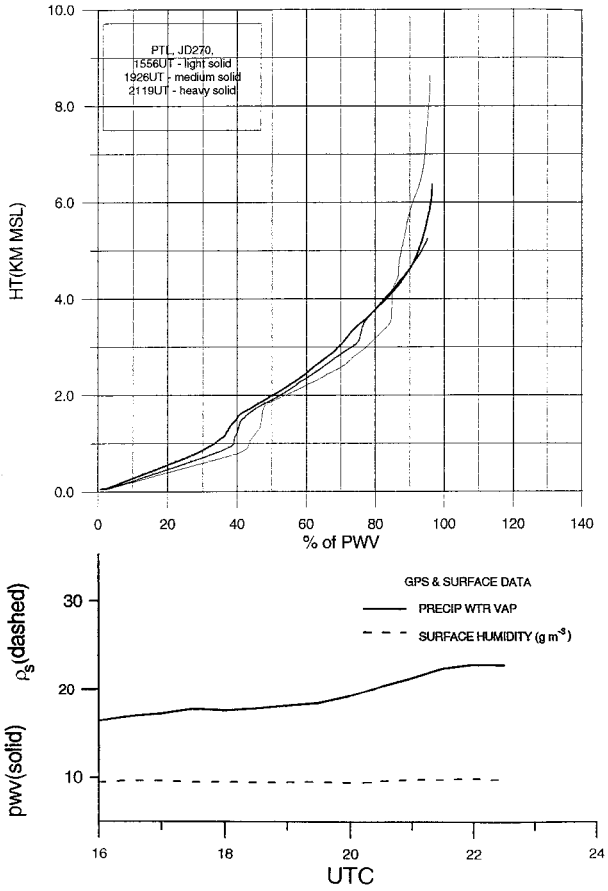

FIG. 3. (top) Cumulative precipitable water vapor vs height in the balloon soundings shown in Fig. 1. (bottom) Temporal records of PWV (solid) and surface value of ρ_V (dashed).

function from pairs of opposing radial velocities (after reversing the velocity scale of one of the two radial spectra). This technique is especially effective for suppressing spectral components that are poorly correlated between beams, such as aircraft, birds, and surface traffic, which were severe contaminants in the Point Loma, California, data. Because clutter is highly correlated on all beams, other techniques were needed for clutter suppression.

To test the limiting accuracy of the technique, we performed a simulation in which we assumed that the humidity gradients found by the radar had the sign of the corresponding layer in the balloon sounding.

To find the total PWV in the height range of penetration of the profiler, we reduced the GPS PWV by the percentage found from the three radiosonde observations (raob's) (about 41% at a height of 1.6 km in Fig. 3) below the greatest height for which the signal-to-noise ratio of the wind profiler and its RASS system are usable. The humidity profiles are then found by constraining the total PWV to that deduced from the GPS and starting the profile with the surface-measured value of ρ_V. The results are shown in Figs. 4–6 for the times of the three soundings. The top frames show the profiles of humidity found by simply integrating the gradient profiles starting with the observed surface value of ρ_V.

Although the top frames resemble the balloon-measured profiles in shape, the results are clearly not accurate enough to be of practical use. The lower frame shows the same case with the integrated profile constrained to the observed total found from the observed value of PWV from GPS. To illustrate the importance of the sign ambiguity, we show in the lower center frame of Fig. 5 (the 1926 UTC sounding) the profile that would have resulted if the sign of the upper gradient (above 1.4 km) had been assumed to be negative, like the sign of the lower layer.

The 1556 UTC sounding shows very strong gradients in both temperature and humidity (and therefore refractive index) at a height of about 900 m. The midday gradients are less strong, and the afternoon gradients are weaker still, so a fairly satisfactory range of conditions is represented. All soundings show a zone of increasing humidity at about 1.4–2-km altitude. The balloon profiles are dashed, and the three cycles of profiler humidity are shown as points joined by solid lines with light to heavy symbols, proceeding from cycle 1 (light) to cycle 3 (heavy). The sounding data are processed up to a height of 1.6 km. The RASS signal is lost at about 1.4 km, and the radar signals become very weak above 1.6 km. Above the RASS penetration, we used the balloon temperature to extend the analysis to a height of 1.6 km.

The agreement between the radar and balloon data is very satisfactory for temperature and for humidity if the sign of the gradients is taken from the balloon sounding. However, in practice, the sign of the humidity gradient in the layers is not known.

5. Applications

In general, humidity decreases with height in the atmosphere; therefore, its height gradients are usually negative. However, the exceptions, such as frontal interfaces, are often important cases. The applicability of the technique therefore seems to be limited to the following three possibilities: 1) operation of profilers near a weather office where meteorologists can identify zones of negative gradient from the synoptic situation; 2) use of the squared gradients provided by the profilers as inputs into models without specifying the sign (that is, the models deduce the sign); and 3) (perhaps the most generally applicable procedure) use of profilers to interpolate and extrapolate between the occasional balloon profiles (usually one every 12 h) in order to obtain a greater temporal density of humidity profiles and to reveal short-term fluctuations.

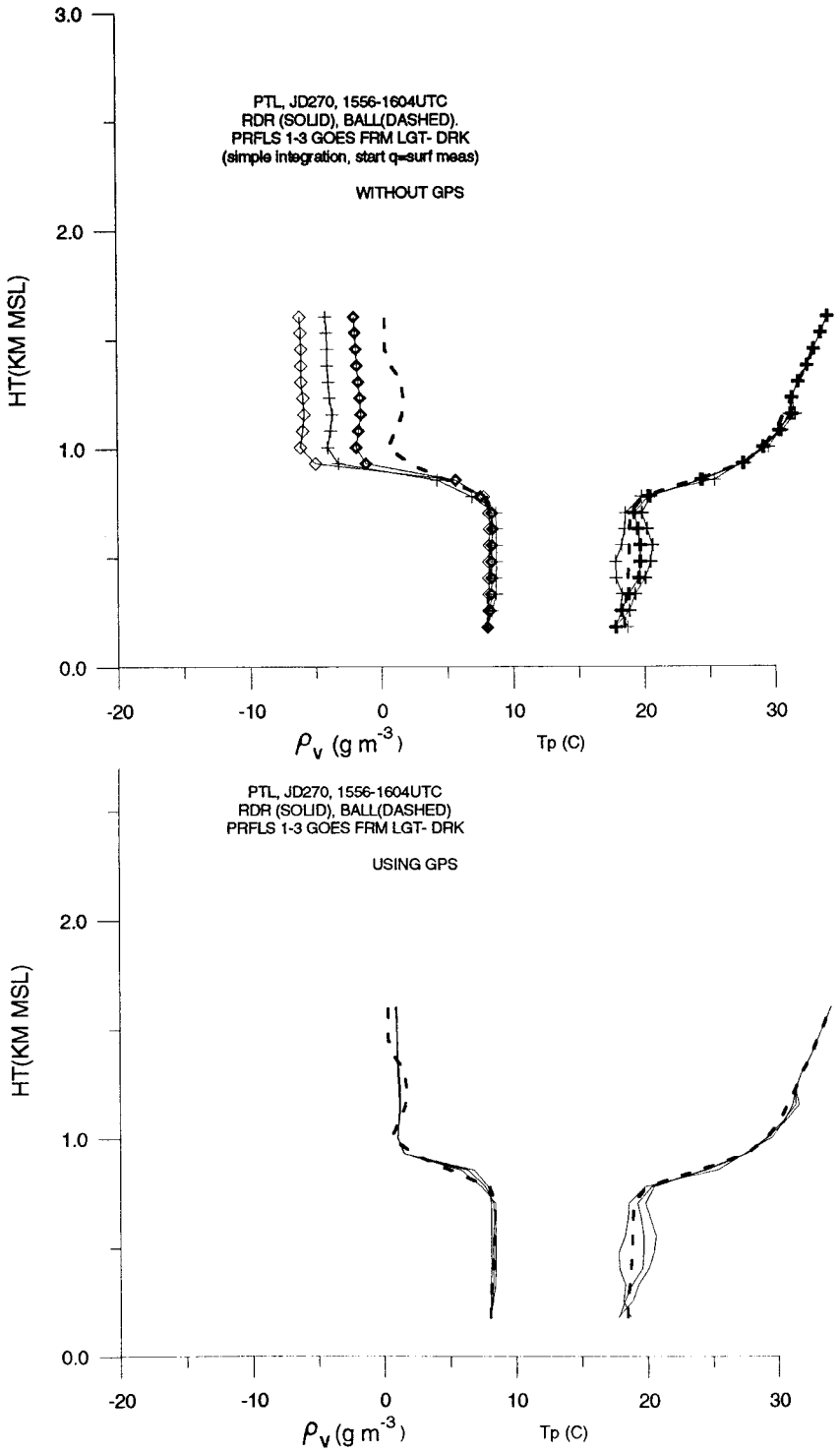

FIG. 4. Balloon-measured humidity profiles (dashed) from the launch at 1556 UTC compared with the radar-measured humidity profiles (solid) deduced from the three cycles of the profiler through five beams during the 10 min required for the balloon to traverse the 1.6-km height range. The ceilometer shows a thin layer of stratus at the inversion base. (top) Simple integration of the gradients of ρ_v found from N_p in (1). (bottom) Same as top panel except the integrations are constrained to yield the PWV measured by GPS. In the integration the sign of the humidity gradient was chosen to be the same as the sign in the balloon sounding. The temperature profiles measured by RASS are shown in the right-hand frames. The RASS soundings reached only 1.4 km in this event, so the balloon temperature is used above that height.

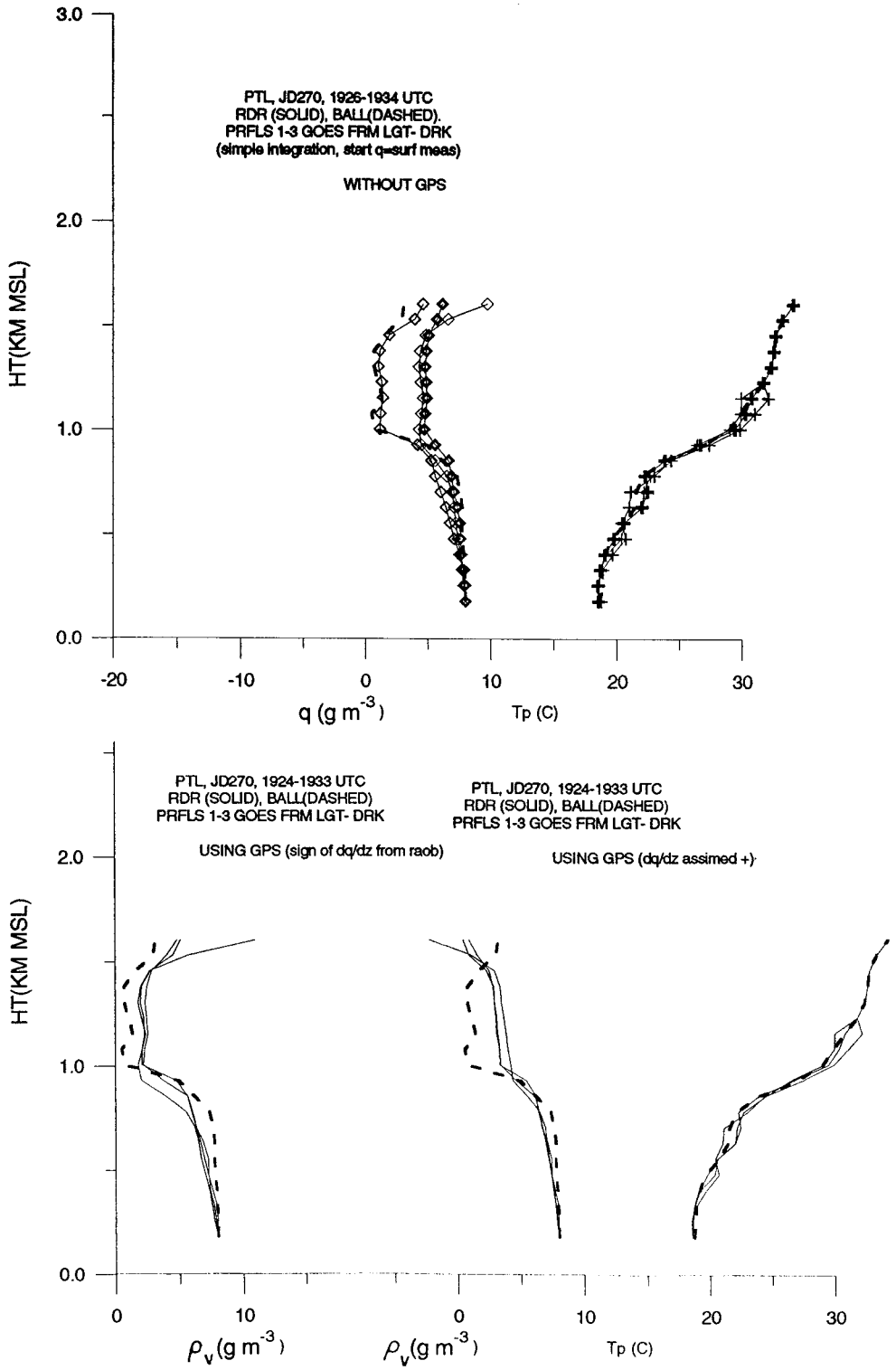

FIG. 5. Same as Fig. 4 except the balloon launch time was 1926 UTC and there were no clouds. The bottom center frame should be compared with the left-hand frame. The center frame shows the profile that would have resulted if the humidity gradient had been chosen always to be negative.

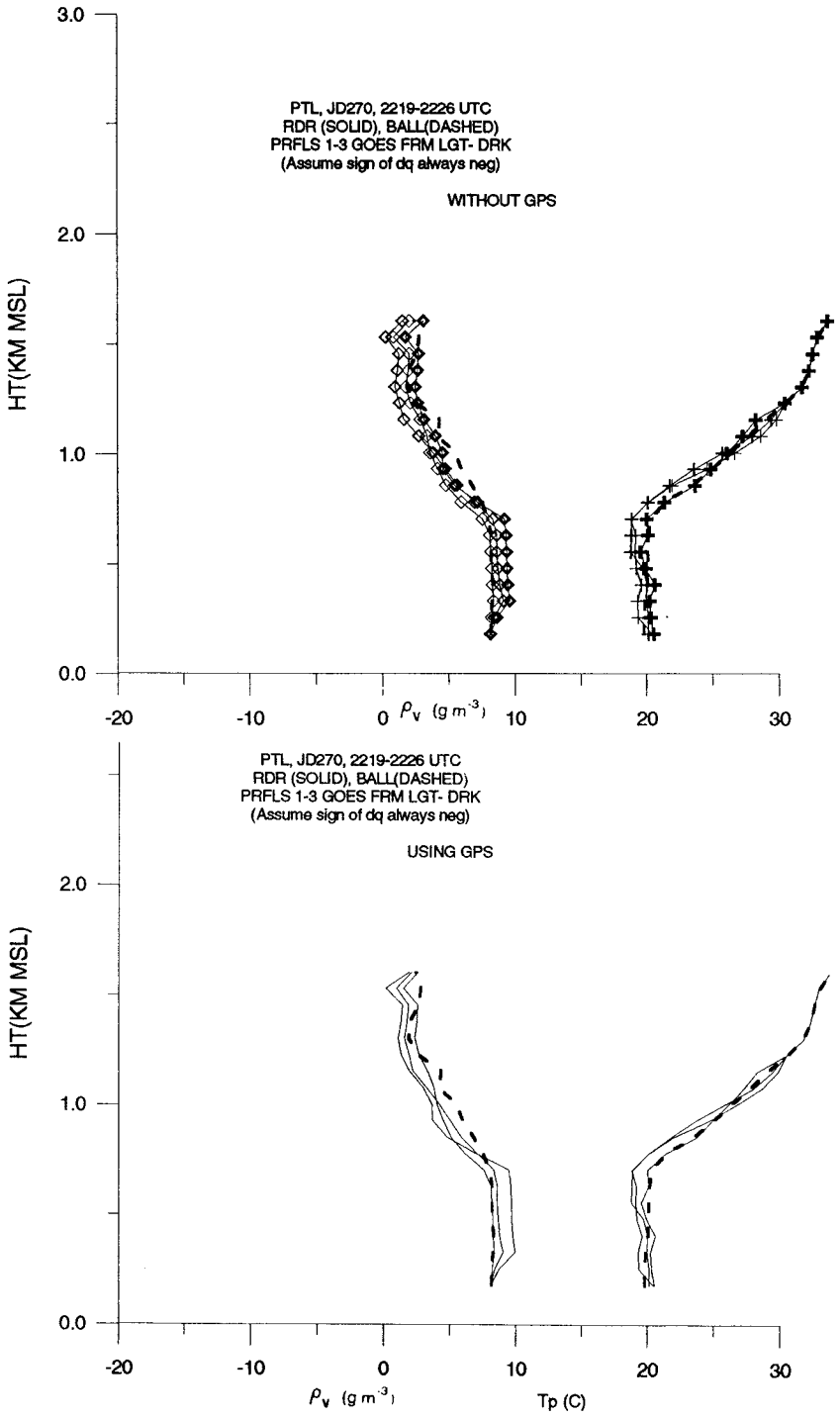

FIG. 6. Same as Fig. 5 except the balloon launch time was 2219 UTC.

6. Discussion

We compared the retrieval of humidity profiles by statistical inversion with the direct integration technique reported here. For the 1556 UTC sounding, the retrieval is shown in Fig. 7. The linear statistical inversion technique was used to estimate atmospheric humidity from a combination of measurements as

$$\rho_V(z) = c_0(z) + \sum_{i=1}^{m} \mathbf{c}_i(z)\mathbf{x}_i, \qquad (2)$$

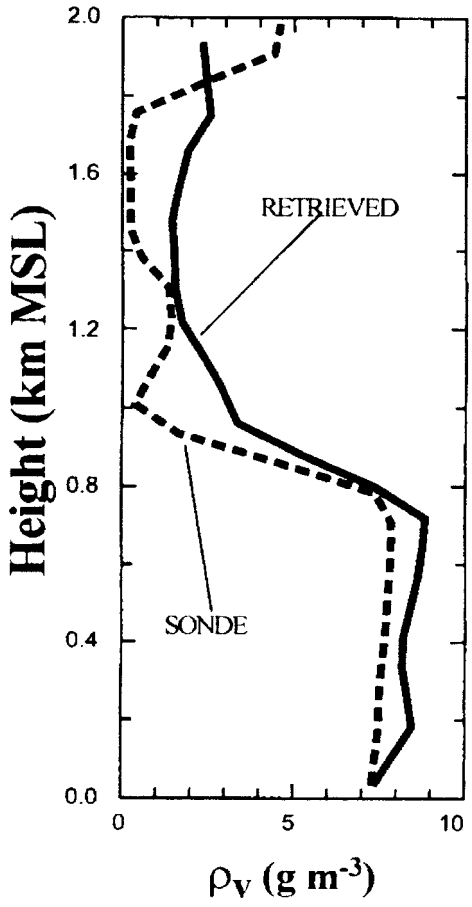

FIG. 7. The method of statistical retrieval described by Stankov et al. (1996) applied to the case shown in Fig. 4. The a priori dataset consisted of 15 years of National Weather Service radiosonde observations during the month of September at San Diego (not far from the Point Loma radar site). The data vector consisted of the 449-MHz profiler measurements of $d\rho_V/dz$ found from (1); the surface values of ρ_V; and the GPS-measured, path-integrated water vapor. At this time there were stratus clouds, and the ceilometer-measured cloud base was also used. The sign of $d\rho_V/dz$ is taken from the balloon (sonde) profile.

where ρ_V is the humidity estimate, z is the height coordinate, m is the number of measurements, $\mathbf{x}_i$ is the measurement vector, and $\mathbf{c}_i$ is the retrieval coefficient vector. An a priori radiosonde dataset for a 15-yr period that is independent of the measurement vector determines the retrieval coefficient vector $\mathbf{c}_i$. This a priori dataset characterizes the site climatology; it consists of San Diego radiosonde ascents for August and September of 1981–95. The measurement vector $\mathbf{x}_i$ consisted of surface meteorological data, a ceilometer, and GPS measurements. This retrieval method falls into the category of a priori linear statistical methods, for which the moisture profile is estimated by (2). The data vector consisted of the 449-MHz profiler measurements of $d\rho_V/dz$ found from (1); surface values of ρ_V; and the GPS-measured, path-integrated water vapor. At 1566 UTC there were stratus clouds, and the ceilometer-measured cloud base was also used as a constraint in the retrieval. The agreement between Figs. 4 and 7 seems encouraging for both methods. Both require independent knowledge of the sign of the gradients because the sign is important in calculating correct profiles.

In these data the greatest departure of the radar-deduced profiles from the balloon-sensed profiles is in the marine mixed layer. Part of the discrepancy may be simply related to fact that the balloon is launched from a land site into a basically marine air mass, and the early sounding may be dominated by the balloon's horizontal trajectory rather than the height distribution of properties. For example, in two of the three soundings humidity *increases* with height in the surface layer, and this positive sign for the gradient is used in the radar retrieval (even though not typically observed). Note that the theoretical basis for (1) requires a statically stable environment because we use the energy equation for a stable atmosphere.

In the zone from 500 to 800 m on the 2219 UTC sounding, two of the three profiler cycles show layers of substantially *higher* humidity than the balloon sounding. To examine the reason for this discrepancy, we look at the profiles of C_N^2, and it is immediately evident that there are strange bulges in two of the three C_N^2 profiles at a height of about 300 m. In the locale of the experiment (a sea coast), this kind of bulge is probably produced by birds since it is low in the soundings and is in only two of the profiles, instead of three, as might be expected from a ubiquitous layer of insects. Bird contamination is an annoying factor in wind retrieval, but, in general, this problem can be minimized by a variety of techniques (Wilczak et al. 1995).

Simple integration leads to profiles that resemble well the balloon profiles in shape but are usually progressively displaced from them with increasing height (see Figs. 4–6). Constraining the total PWV to the GPS value brings the radar and balloon profiles into good agreement by effectively yielding a modified value of L_w/L_N (found to be about 4 by GWMPAR). The modifying factor found from GPS typically lies between 0.5 and 1.5 in these data. Figure 8, taken from GWMPAR, shows measurements of the two length scales versus height. The variable L_w is calculated from radar-measured values of C_w^2 and radar-measured wind shear. The variable L_N is found from the radar-measured C_N^2 and the balloon-measured gradient of potential refractive index. Like the Richardson number, there is much scatter but patterns are clear. Both scales become very small in the stable layer and large in zones of near-neutral stability. A median value of their ratio is about 4, and a solid curve of L_N multiplied by 4 is shown superimposed on the L_w points in Fig. 8. The modification of the ratio required for matching the PWV from GPS may result from the inherent noisiness of the measurements of such factors as shear squared and turbulence intensity.

GWMPAR showed that the outer scales, as defined here, become very small under very stable conditions.

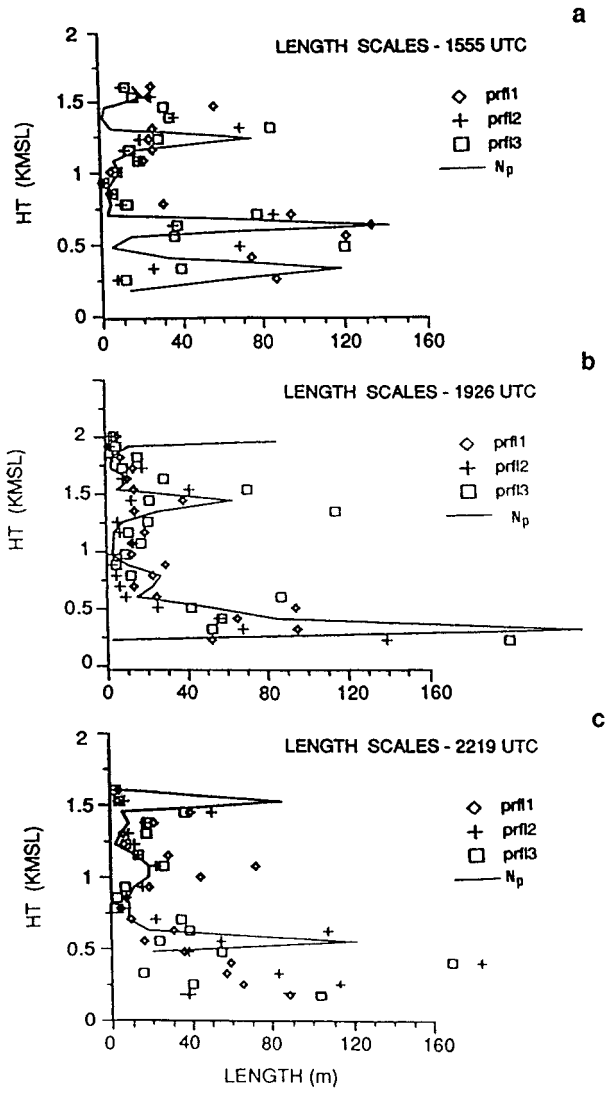

FIG. 8. Length scales calculated for the three successive radar cycles during the three balloon soundings shown in Fig. 2. The points represent the length scale of the vertical velocity. The solid curve represents the length scale of N_p multiplied by 4. It was calculated from the average C_N^2 that was measured by the radar and the gradient of N_p that was measured by balloon to illustrate the goodness of fit for a ratio of length scales equal to 4.

In fact, near the center of the layer they can be smaller than the dimensions of the pulse volume. Anisotropy may also influence the modification factor within such layers, but more work will be needed to properly isolate these effects.

Acknowledgments. The authors wish to express their appreciation for the support, encouragement, and advice of Russell B. Chadwick, Seth Gutman, Rich Lataitis, Ken Moran, M. J. Post, Richard Strauch, and Brian Templeman. This work was partially supported by the Naval Command Control and Ocean Surveillance Center (J. H. Richter, contract monitor).

REFERENCES

Bean, B. R., and E. J. Dutton, 1966: *Radio Meteorology, National Bureau of Standards Monogr.*, No. 92, U.S. Govt. Printing Office, 435 pp.

——, R. E. McGavin, R. B. Chadwick, and B. B. Warner, 1971: Preliminary results of utilizing the high-resolution FM radar as a boundary-layer probe. *Bound.-Layer Meteor.*, **1,** 466–473.

Chadwick, R. B., and E. E. Gossard, 1983: Radar remote sensing of the clear atmosphere—Review and applications. *Proc. IEEE,* **71,** 738–753.

Gage, K. S., and B. B. Balsley, 1980: On the scattering and reflection mechanisms contributing to clear air echoes from the troposphere, stratosphere, and mesosphere. *Radio Sci.,* **15,** 243–257.

Gossard, E. E., and R. G. Strauch, 1983: *Radar Observations of Clear Air and Clouds.* Elsevier, 280 pp.

——, R. B. Chadwick, W. D. Neff, and K. P. Moran, 1982: The use of ground-based Doppler radars to measure gradients, fluxes, and structure parameters in elevated layers. *J. Appl. Meteor.*, **21,** 211–226.

——, D. E. Wolfe, K. P. Moran, R. A. Paulus, K. D. Anderson, and L. T. Rogers, 1998: Measurement of clear-air gradients and turbulence properties with radar wind profilers. *J. Atmos. Oceanic Technol.,* **15,** 321–342.

Ottersten, H., 1969: Atmospheric structure and radar backscattering in clear air. *Radio Sci.,* **4,** 1179–1193.

Richter, J. H., and E. E. Gossard, 1970: Lower tropospheric structure as seen by a high-resolution radar. Tech. Rep. NELC/TR 1718, Naval Command Control and Ocean Surveillance Center, San Diego, CA, 66 pp.

Stankov, B. B., E. R. Westwater, and E. E. Gossard, 1996: Use of wind profiler estimates of significant moisture gradients to improve humidity profile retrieval. *J. Atmos. Oceanic Technol.,* **13,** 1285–1290.

Tatarskii, V. I., 1961: *Wave Propagation in a Turbulent Medium.* McGraw-Hill, 285 pp.

——, 1971: The effects of the turbulent atmosphere on wave propagation. NTIS TT 68-50464, Israel Program for Scientific Translations, Jerusalem, Israel, 472 pp. [Available from the National Technical Information Service, 5285 Port Royal Rd., Springfield, VA 22161.]

VanZandt, T. E., J. L. Green, K. S. Gage, and W. L. Clark, 1978: Vertical profiles of refractivity structure constant: Comparison of observations by the Sunset radar with a new theoretical model. *Radio Sci.,* **13,** 819–829.

Wilczak, J. W., and Coauthors, 1995: Contamination of wind profiler data by migrating birds: Characteristics of corrupted data with potential solutions. *J. Atmos. Oceanic Technol.,* **12,** 449–467.

Wolfe, D. E., B. L. Weber, D. B. Wuertz, and K. P. Moran, 1997: The California Air Resources Board 1995 Mojave Desert Ozone Experiment. NOAA Tech. Memo. ERL ETL-273, NOAA/Environmental Technology Laboratory, Boulder, CO, 96 pp. [Available from the National Technical Information Service, 5285 Port Royal Rd., Springfield, VA 22161.]